PAPER

Enhanced photomechanical response of a Ni–Ti shape memory alloy coated with polymer-based photothermal composites

IOP Publishing Smart Materials and Structures
Smart Mater. Struct. **26** (2017) 105012 (7pp) https://doi.org/10.1088/1361-665X/aa80cb

Enhanced photomechanical response of a Ni–Ti shape memory alloy coated with polymer-based photothermal composites

M G Perez-Zúñiga, F M Sánchez-Arévalo and J Hernández-Cordero

Instituto de Investigaciones en Materiales, Universidad Nacional Autónoma de México, Apdo.Postal 70-360, Ciudad Universitaria, Cd. Mx 04510, México

E-mail: jhcordero@iim.unam.mx

Received 16 May 2017, revised 15 July 2017
Accepted for publication 19 July 2017
Published 1 September 2017

Abstract

A simple way to enhance the activation of shape memory effects with light in a Ni–Ti alloy is demonstrated. Using polydimethylsiloxane-carbon nanopowder (PDMS+CNP) composites as coatings, the one-way shape memory effect (OWSME) of the alloy can be triggered using low power IR light from a laser diode. The PDMS+CNP coatings serve as photothermal materials capable to absorb light, and subsequently generate and dissipate heat in a highly efficient manner, thereby reducing the optical powers required for triggering the OWSME in the Ni–Ti alloy. Experimental results with a cantilever flexural test using both, bare Ni–Ti and coated samples, show that the PDMS+CNP coatings perform as thermal boosters, and therefore the temperatures required for phase transformation in the alloy can be readily obtained with low laser powers. It is also shown that the two-way shape memory effect (TWSME) can be set in the Ni–Ti alloy through cycling the TWSME by simply modulating the laser diode signal. This provides a simple means for training the material, yielding a light driven actuator capable to provide forces in the mN range. Hence, the use of photothermal coatings on Ni–Ti shape memory alloys may offer new possibilities for developing light-controlled smart actuators.

Supplementary material for this article is available online

Keywords: shape memory alloys, photothermal effects, polymer coatings, laser heating, fiber optics

(Some figures may appear in colour only in the online journal)

1. Introduction

The continuous evolution of materials science and engineering relies on developing novel materials with new and improved attributes. As an example, the nickel–titanium (Ni–Ti) shape memory alloy (SMA) belongs to a class of complex materials showing interesting thermomechanical effects. These include the one-way shape memory effect (OWSME), the super-elastic effect, and the well-known two-way shape memory effect (TWSME) [1, 2]. Although these effects have been extensively studied, there are still persistent efforts to improve the extraordinary properties of these materials; moreover, special interest has been focused on the shape memory triggering mechanisms. Conventional ways to obtain the shape memory effect (SME) include temperature changes, stress, exposure to magnetic fields, or a combination of these [3, 4]. In metallic alloys, the SME is more commonly reached by temperature or stress [5], although new alternatives such as laser irradiation have been explored as well. This interesting option for triggering thermomechanical effects in Ni–Ti SMA is based on heating through laser irradiation [6, 7], thus offering the possibility of remotely modifying the shape of Ni–Ti elements and allowing for the development of light activated actuators [8–10].

Laser triggering of thermomechanical effects in SMA is based on optical absorption, heat generation and dissipation within the alloy. In order to initiate the desired SMEs, the appropriate temperatures for phase transformation must be

reached in a controlled fashion. The optical absorption features of the material and subsequent heat generation required for these purposes can be improved upon using adequate optical coatings on the Ni–Ti SMA. Hence, the optical and thermal properties of the coatings are very important to obtain adequate light absorption to increase the temperature in the alloy. Multilayer optical filters deposited directly on the SMA surface have shown to be useful for selective activation of SMA alloys [6, 7]. Albeit providing wavelength selective activation of SMA elements, this approach requires elaborated fabrication procedures for depositing alternate layers of different composite materials. Moreover, some additional optical elements such as micro-lenses are needed in order to focus the light and reach the appropriate phase transformation temperatures. Some shape memory polymers can also be activated by light irradiation [11], and their performance can be readily enhanced using carbon-based fillers [12]. However, the actuation force produced with these materials is limited due to their own nature.

In this work, a novel and simple way to trigger SMEs with light was explored. The basic idea behind this approach is to improve laser light absorption and subsequent heat release on Ni–Ti samples. This is achieved upon coating the SMA with a polymer-based photothermal membrane, capable to generate highly localized heat via infrared (IR) light absorption [13–16]. The composite membranes are fabricated using carbon nanopowder (CNP) hosted by a polydimethylsiloxane (PDMS) matrix thus yielding a highly efficient photothermal material [16]. Owing to their ease of processing and flexibility, these photothermal composites can be simply incorporated onto Ni–Ti SMA with different shapes. The effects of these composites on the mechanical actuation exhibited by Ni–Ti sheets when irradiated with an IR laser diode were explored. Experimental results show that the photothermal coatings allow for reaching the critical phase transformation temperatures of the smart composite using low power laser irradiation, thus offering a new and versatile means to activate SMEs with minimum contact.

2. Experimental details

2.1. Sample preparation

A commercially available equiatomic Ni–Ti alloy, presenting a mixture of austenitic and martensitic phases at room temperature, was used as received. The critical temperatures for phase transformation ($M_s = 3.2\,^{\circ}\mathrm{C}$, $M_f = -6.2\,^{\circ}\mathrm{C}$, $A_s = 38\,^{\circ}\mathrm{C}$ and $A_f = 43\,^{\circ}\mathrm{C}$) were determined by differential scanning calorimetric (DSC) measurements, using a DSC Q100 equipment from TA Instruments at a temperature rate of $10\,^{\circ}\mathrm{C\,min^{-1}}$ during the heating and cooling cycles. Coatings with photothermal features were obtained upon mixing the CNP with the PDMS following the procedures reported elsewhere [16]. The photothermal properties of these polymer-carbon (PDMS+CNP) composites depend on the dispersion and cluster formation of CNP within the polymer matrix. Two types of coatings were used: one favouring heat generation (labeled as composite $C1$), and another one favouring heat conduction (labeled as composite $C2$). Such capabilities depend on cluster formation within the composite, and this can be adjusted during the fabrication process (see [16] for details). Both composites were fabricated using a concentration of 0.1% in weight of CNP (particle size <100 nm, Sigma Aldrich 633100) compared to the total amount of PDMS (Dow Corning, Sylgard 184). The PDMS +CNP mixtures were poured into a glass mold and cured at 80 °C during 2 h. This procedure yields membranes with a thickness of 420 μm, which were subsequently cut in square samples of 2 mm.

The heating performance of the coatings was evaluated using a Fluke Ti300 IR thermal camera, setting the emissivity coefficient $\beta = 0.74$, as commonly done for Ni−Ti surfaces [17]. Thermal images were acquired from the surface of the SMA sample under different laser irradiation conditions. This allowed us to register the increase in temperature at the surface of the Ni–Ti alloy as a function of the optical intensity ($I = \frac{P_0}{\pi w_0^2}$, $w_0 =$ laser spot radius) impinging on the opposite surface of the samples. The laser source used to irradiate the membranes was an IR fiber coupled laser diode ($\lambda = 975$ nm), and the range of optical power (P_0) used for our experiments was from 8 to 270 mW. In order to evaluate the influence of the PDMS+CNP on the activation of the SME, the polymer coatings were placed on the surface of a Ni–Ti narrow beam using a thin layer of thermal paste to provide adequate thermal contact even during the change of shape of the alloy. The laser triggering capabilities of three different samples (Ni−Ti, Ni–Ti + $C1$ and Ni–Ti + $C2$) were then evaluated as described in the following section.

2.2. Laser triggering of mechanical actuation

A cantilever beam arrangement was used to evaluate the mechanical actuation of the samples triggered by IR irradiation. The relevant measurements were based on the superelastic effect of the SMA [18]. Narrow beams with dimension of $13 \times 1.6 \times 0.1$ mm (length, width and thickness, respectively) were cut from the Ni–Ti sheet. Each sample was mechanically tested using a custom-designed device to register the relevant parameters involved in the bending test (see figure 1(a)). These were registered using a virtual instrument (VI) programmed in LabVIEW, capable to simultaneously acquire data such as time, displacement, force and images during the experiments. While the beam deflection was controlled through the VI, the displacement and applied force (F) at the free end of the beam were measured by a LVDT (Lucas Schaevitz MHR-1000) and a precision miniature load cell (Honeywell, model 34), respectively. The cantilever beam was displaced 8 mm in steps of 0.5 mm; as a result, the normal stress (σ)—close to the grip region—increased gradually until reaching the critical stress value (σ_c) required to induce the martensitic phase. As depicted in figure 1(b), this approach allows to obtain well-defined martensitic regions where $\sigma \geqslant \sigma_c$. The stress versus strain curves for the samples were obtained using the acquired data and beam theory [19]. The critical stress value for transformation (σ_c), accountable

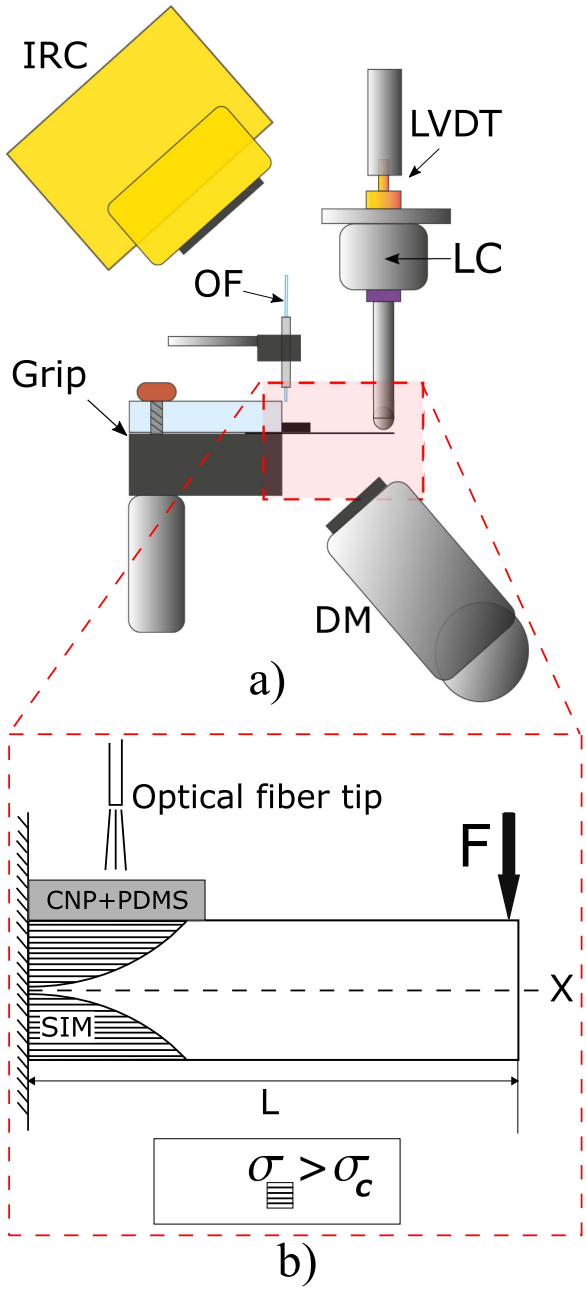

Figure 1. Experimental setup used to evaluate the mechanical response of Ni–Ti SMA activated by IR irradiation. (a) Mechanical tester: IR thermal camera (IRC), optical digital microscope (DM), load cell (LC), displacement sensor (LVDT), optical fiber (OF); (b) detail of cantilever beam of Ni–Ti alloy coated with PDMS + CNP under bending.

for the significant changes in the slopes of the stress versus strain superelastic loops, were determined as well.

Bending measurements were conducted with the bare (Ni–Ti) and coated (Ni–Ti + $C1$, Ni–Ti + $C2$) beams under similar condition of laser irradiation. The temperature reached for each case varied depending on the photothermal features of coatings $C1$ and $C2$. Because of the improved optical absorption of the coatings, the temperature in the vicinity of the irradiated area increases until reaching values above $A_f = 43$ °C. With our setup, the spot size of the laser beam

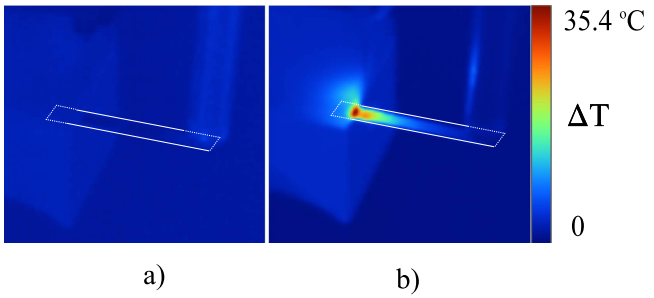

Figure 2. IR thermal camera images showing the registered increase in temperature ΔT (°C); (a) Ni–Ti beam without laser irradiation, (b) Ni–Ti beam irradiated with an optical intensity of 453 mW mm $^{-2}$.

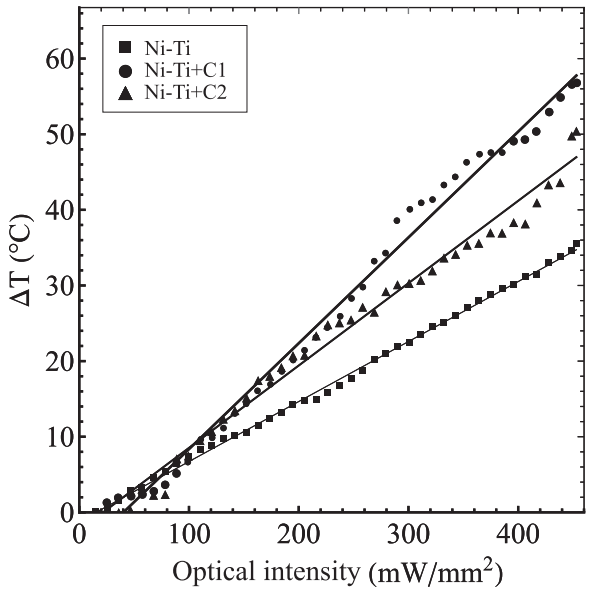

Figure 3. Maximum temperature increase (ΔT) measured in the Ni−Ti samples with the IR camera as a function of optical intensity. The slopes of the linear fittings (solid lines) for the experimental data points are 0.08 °C mW^{-1} mm^{-2} for the bare sample (Ni–Ti), while the coated samples yield values of 0.14 °C mW^{-1} mm^{-2} (for Ni–Ti + $C1$) and 0.1 °C mW^{-1} mm^{-2} (for Ni–Ti + $C2$).

can be adjusted upon moving the optical fiber located above the fixed end of the Ni–Ti beams. For all experiments, the fiber end face was placed at a fixed distance of 3 mm above the Ni–Ti beam, yielding a spot area of approximately 0.6 mm^2 ($w_0 = 434$ μm). In addition, the bending test was continuously recorded with a digital microscope (DinoLite) and the IR thermal camera (see figure 2(a)) which was also used for temperature monitoring on the surface of all the samples, as seen in figures 2(a) and (b).

3. Results

3.1. Heating performance of the coatings

The results shown in figure 3 confirm that for all the samples, an increase in temperature is achieved through IR laser irradiation. As seen in the figure, the registered increase in temperature ΔT in all cases is linearly proportional to the

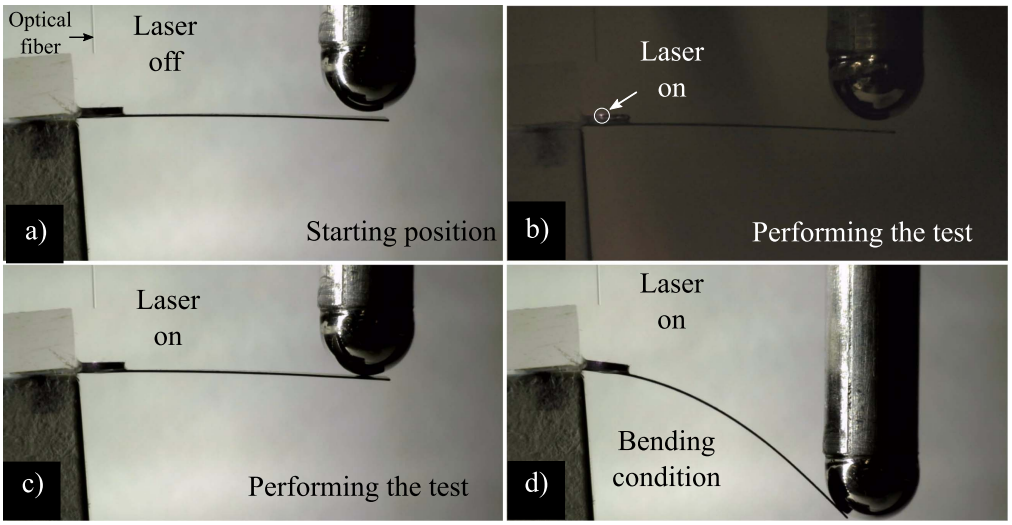

Figure 4. Bending test on the Ni–Ti cantilever beam: (a) starting position (laser off) for the loading process; (b) image acquired with different contrast settings to show the laser spot on the coating; (c) during the test, the laser is turned on to heat the sample as the actuator starts to apply force on the free end of the beam; (d) final stage of the loading process showing a displacement of 8 mm; the unloading process is carried out following the opposite sequence until the beam reaches the initial position.

optical intensity. In agreement with previous reports [16], these results further show that coatings $C1$ and $C2$ present different heat generation capabilities, as observed from the ΔT versus optical intensity curves shown on figure 3. The slope of each curve represents the photothermal performance of the coating: while the coating with higher slope ($C1$) shows improved heating capabilities, the other coating ($C2$) provides better heat dissipation features [16]. The photothermal response of the coatings were as follows: $C1$ yielded a slope of 0.14 °C $\text{mW}^{-1}\,\text{mm}^{-2}$, yielding a maximum ΔT (56.7 °C) for the maximum optical power available from the laser diode (270 mW); $C2$ showed a 0.1 °C $\text{mW}^{-1}\,\text{mm}^{-2}$ slope and a $\Delta T = 50.6$ °C. Meanwhile, the bare Ni–Ti alloy yielded a slope of 0.08 °C $\text{mW}^{-1}\,\text{mm}^{-2}$ and a maximum increase in temperature $\Delta T = 35.4$ °C. According to these results, and considering the slope $\frac{d\Delta T}{dI}$ of the bare Ni–Ti as a reference, an enhancement in heating performance of 60% and 43% was obtained for $C1$ and $C2$, respectively. Note that these enhancements are more evident for optical intensities above 300 mW mm^{-2}. This result becomes important for achieving the temperature required to induce the martensitic to austenitic phase transformation in the SMA, because a lower optical intensity will be needed to trigger the SME when using the photothermal coatings.

3.2. Thermomechanical response

The thermomechanical response of the samples was evaluated performing a cantilever beam bending test, as shown in figure 4. As required by beam theory [19], the geometry of the beam (length, width and thickness), the applied force and the displacement at the end of the cantilever beam were used to calculate the normal stress and its associated strain during the test. The resulting stress versus strain (σ versus ε) curves for each sample are shown in figure 5; these were obtained under similar laser irradiation conditions, yielding different temperatures owing to the different photothermal performances of the bare and coated beam samples. For the bare Ni−Ti beam, the expected superelastic loop during the loading and unloading processes was observed (figure 5(a)). At room temperature (25.6 °C), the mechanical behavior of the Ni–Ti sample involves a mixture of austenite and martensite phases resulting in a critical stress $\sigma_c = 120$ MPa. When irradiated with the laser at optical intensities of 94.7 and 453 mW mm^{-2}, the temperature registered at the fixed end of the beam increased up to 39.8 and 61 °C, and the flexural test yielded values of $\sigma_c = 193.5$ and $\sigma_c = 194$ MPa, respectively. As expected, an increase in temperature modifies the mechanical response of bare Ni−Ti sample [2]; notice that for temperatures above $A_f = 43$ °C, the sample will present only the austenite phase within the laser heated region. Hence, for a fixed value of temperature above A_f, stress induced martensitic transformation can be obtained if $\sigma > \sigma_c$.

Figures 5(b) and (c) show the mechanical responses obtained from the Ni–Ti + $C1$ and Ni–Ti + $C2$ samples. The room temperature registered during the test with the Ni–Ti + $C1$ was 28.8 °C, and under laser irradiation the temperature was measured to reach values of 49.0 and 85.5 °C for optical intensities of 194.7 and 453 mW mm^{-2}, respectively. The resulting critical stresses (σ_c) for each case were correspondingly 137.6, 208.3 and 225.8 MPa. Meanwhile, for the Ni–Ti + $C2$ the room temperature was 28.7 °C and the temperatures reached under laser irradiation were 49.5 and 79.2 °C, yielding values for σ_c of 126.2, 211.8 and 217.8 MPa, respectively. Note that these temperatures were attained with the same optical intensities as those used for the previous sample. Hence, under the same irradiation conditions, the temperature reached at the fixed end of the beam will vary depending to the photothermal features of the coating.

Considering the heating performance and the thermomechanical response, the coating labeled as $C1$ exhibited the best photothermal features to trigger the SME in a controlled

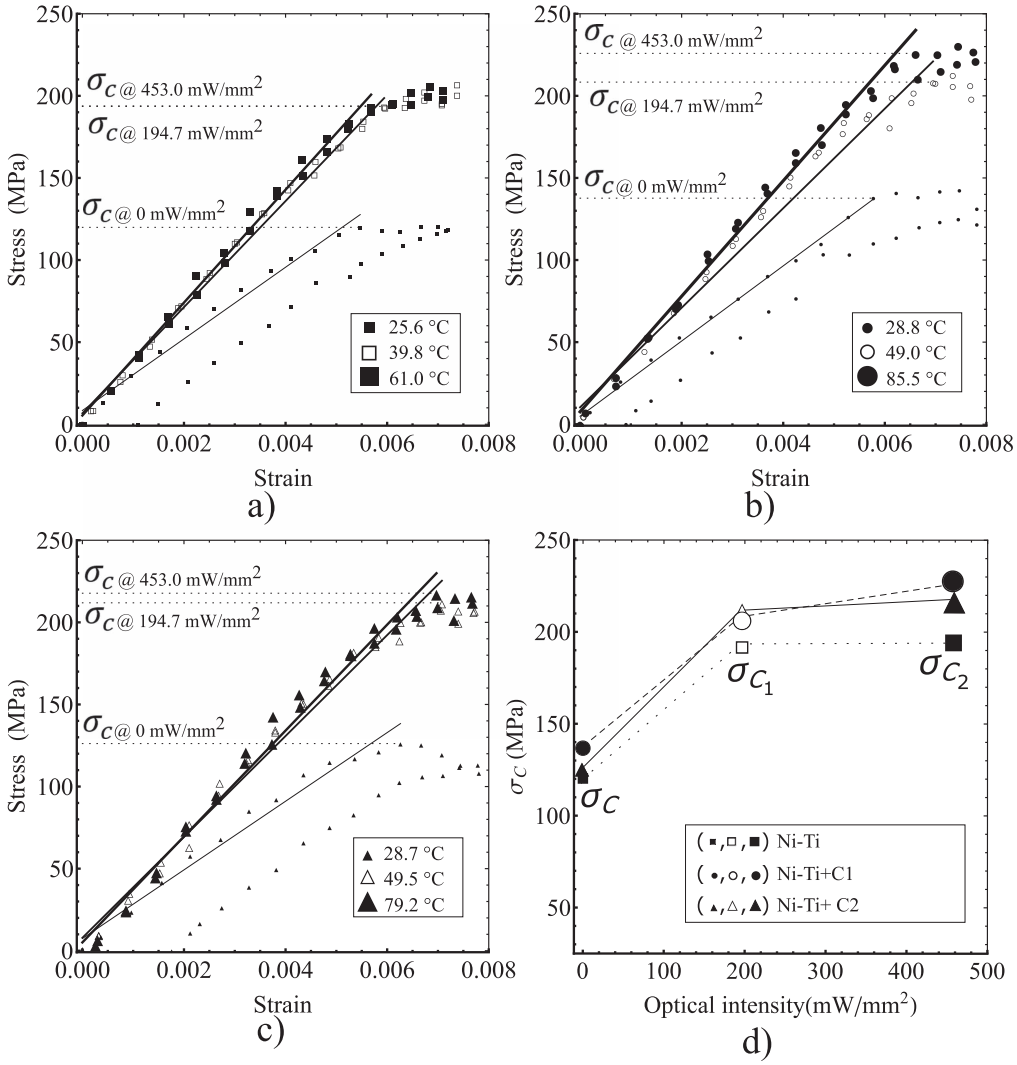

Figure 5. Thermomechanical response of the bare and coated Ni−Ti samples tested at different IR optical intensities. (a) Bare sample, (b) Ni–Ti + $C1$ sample, (c) Ni–Ti + $C2$. The critical stresses shown in (d) indicate that the best performance for the maximum optical intensity is obtained using the coating labeled as $C1$.

Table 1. Maximum increase in temperature and corresponding critical stress transformation values for the different Ni−Ti samples. All data were obtained for the same optical intensity ($I = 453$ mW mm^{-2}).

Sample	ΔT_{max} (°C)	σ_c (MPa)	Increase in σ_c (%)
Ni–Ti	35.4	194	–
Ni–Ti+C1	56.7	225.8	16
Ni–Ti+C2	50.6	217.7	12

fashion. Enhanced heating of the Ni−Ti samples is thus readily obtained through the improved optical absorption and heat release of the photothermal coatings. Figure 5(d) shows the values for the critical stress obtained for each sample for the temperatures reached at different optical intensities. From these results, it is evident that the photothermal coatings improve the triggering of the mechanical actuation mechanism for the Ni−Ti SMA. Table 1 shows the maximum increase in temperature obtained for the three cases analyzed in our experiments. For comparison, the critical stresses obtained for each case are also included. Notice that an increase in the critical stress value is effectively obtained with the coated samples when compared to the σ_c registered for the bare Ni−Ti SMA.

Finally, the feasibility of setting the TWSME in the Ni–Ti sample using laser irradiation for the training process was explored. This was done at the final stage of the loading process, sustaining the bending condition (see figure 4(d)) and exposing the SMA to temperature cycles upon modulating the laser. According to the critical temperatures for phase transformation obtained for the alloy, and for typical room temperature conditions (approximately 20 °C), the ΔT required for this purpose is only within 20 °C. Such an increase in temperature can be easily achieved through the photothermal effects obtained in our previous experiments. Hence, the laser diode was modulated with a square signal at a frequency of 10 mHz, reaching a maximum optical intensity of 453 mW mm^{-2}; this irradiation conditions thus yielded temperature changes from room temperature to 61 °C. The force

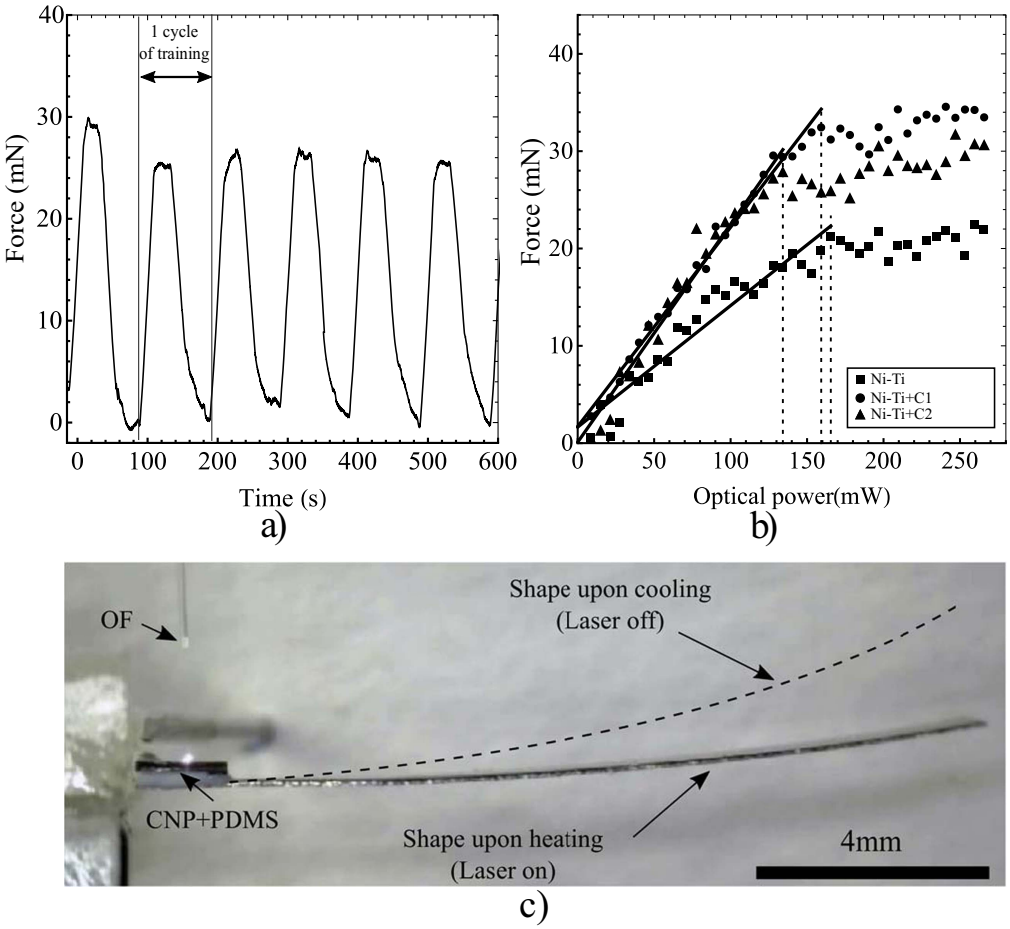

Figure 6. Setting the double shape memory effect (TWSME) on the Ni−Ti sample. (a) Thermomechanical cycling of the sample: force registered by the load cell when the laser diode was modulated at a frequency of 10 mHz; (b) force generated by the bare and coated Ni–Ti samples, after the training process, as a function of the optical intensity; (c) shapes adopted by the beam after training when the laser is turned on and off (see video for details).

registered by the load cell as a function of time during the cycling process is presented in figure 6(a). Under these training conditions, the TWSME was set in the alloy after 250 cycles. The mechanical response as a function of optical intensity resulting from triggering the TWSME in each sample is shown in figure 6(b). As observed from the slopes obtained from these experiments, a lower force generation was obtained for the bare Ni–Ti alloy compared to the coated samples. While the slope for the Ni–Ti alloy was 0.125 $mN\,mW^{-1}$, the coated samples presented very similar slopes of approximately 0.2 $mN\,mW^{-1}$. The maximum force was attained with the sample coated with C1, reaching 32 mN for an optical power of 153 mW, which represents an enhancement of 167% with respect to the bare sample.

4. Conclusions

Highly efficient photothermal coatings on a Ni–Ti alloy have been used to demonstrated a simple means to enhance the activation of the OWSME. The enhanced photothermal features of these coatings allow for triggering the SME with lower IR laser powers compared to those required for bare Ni–Ti samples. We further demonstrated a novel approach to set the TWSME based on cycling the OWSME upon irradiating the alloy with a modulated optical signal. Using this technique, we were able to train the material yielding a light-driven actuator capable to provide a force of approximately 32 mN. Both, the incorporation of the polymer coatings on the alloy, and the optical devices required for this purpose are simple, and thus open new possibilities for developing light-controlled smart actuators or sensors with remote activation capabilities.

Acknowledgments

This work was developed with the financial support from PAPIIT DGAPA-UNAM program through grants IT100215 and IT101215. M G Pérez-Zúniga appreciates financial support from CONACyT during his graduate studies. The authors would like to acknowledge technical support from Adriana Tejeda for X-Ray measurements and Eriseth Morales for DSC characterization.

ORCID iDs

F M Sánchez-Arévalo https://orcid.org/0000-0003-4369-1262
J Hernández-Cordero https://orcid.org/0000-0003-3459-2158

References

[1] Jani J M, Leary M, Subic A and Gibson M A 2014 A review of shape memory alloy research, applications and opportunities *Mater. Des.* **56** 1078–113
[2] Otsuka K and Wayman C M 1999 *Shape Memory Materials* (Cambridge: Cambridge University Press)
[3] García-Castillo F N, Cortés-Pérez J, Amigó V, Sánchez-Arévalo F M and Lara-Rodríguez G A 2015 Development of a stress-induced martensitic transformation criterion for a cu-al-be polycrystalline shape memory alloy undergoing uniaxial tension *Acta Mater.* **97** 131–45
[4] Mohr R, Kratz K, Weigel T, Lucka-Gabor M, Moneke M and Lendlein A 2006 Initiation of shape-memory effect by inductive heating of magnetic nanoparticles in thermoplastic polymers *Proc. Natl Acad. Sci. USA* **103** 3540–5
[5] Sánchez-Arévalo F M, Aldama-Reyna W, Lara-Rodriguez A G, García-Fernández T, Pulos G, Trivi M and Villagran-Muniz M 2010 Use of time history speckle pattern and pulsed photoacoustic techniques to detect the self-accommodating transformation in a cu-al-ni shape memory alloy *Mater. Charact.* **61** 524
[6] Zaidi S, Lamarque F, Favergeon J, Carton O and Prelle C 2011 Wavelength-selective shape memory alloy for wireless microactuation of a bistable curved beam *IEEE Trans. Ind. Electron.* **58** 5288–95
[7] Zaidi S, Lamarque F, Prelle C, Carton O and Zeinert A 2012 Contactless and selective energy transfer to a bistable micro-actuator using laser heated shape memory alloy *Smart Mater. Struct.* **21** 115027
[8] Yamaguchi K, Ono R and Okamura H 2009 Light-driven actuator with energy conversion efficiency in the order of 1 *Appl. Phys. Express* **2** 034502
[9] Avirovik D, Kumar A, Bodnar R J and Priya S 2013 Remote light energy harvesting and actuation using shape memory alloy—piezoelectric hybrid transducer *Smart Mater. Struct.* **22** 5
[10] Hu Z, Kanth B R, Tamang R, Varghese B, Sow C-H and Mukhopadhyay P K 2012 Visible microactuation of a ferromagnetic shape memory alloy by focused laser beam *Smart Mater. Struct.* **21** 032003
[11] Lendlein A, Jiang H, Junger O and Langer R 2005 Light-induced shape-memory polymers *Nature* **434** 879–82
[12] Lu H, Liu Y, Gou J, Leng J and Du S 2010 Synergistic effect of carbon nanofiber and carbon nanopaper on shape memory polymer composite *Appl. Phys. Lett.* **96** 084102
[13] Pimentel-Domínguez R, Sánchez-Arévalo F M, Hautefeuille M and Hernández-Cordero J 2013 Laser induced deformation in polydimethylsiloxane membranes with embedded carbon nanopowder *Smart Mater. Struct.* **22** 037001
[14] Vélez-Cordero J R, Velázquez-Benítez A M and Hernández-Cordero J 2014 Thermocapillary flow in glass tubes coated with photoresponsive layers *Langmuir* **30** 5326–36
[15] Rodrigo Vélez-Cordero J and Hernandez-Cordero J 2015 Heat generation and conduction in pdms-carbon nanoparticle membranes irradiated with optical fibers *Int. J. Therm. Sci.* **96** 12–22
[16] Pimentel-Domínguez R, Velázquez-Benítez A, Vélez-Cordero J, Hautefeuille M, Sánchez-Arévalo F and Hernández-Cordero J 2016 Photothermal effects and applications of polydimethylsiloxane membranes with carbon nanoparticles *Polymers* **8** 84
[17] Zurbitu J, Zabaleta A, Cesari E, Aurrekoetxea J and Kustov S 2010 *Thermo-Mechanical Behaviour of NiTi at Impact* (Rijeka: Intech)
[18] Wayman C M and Duerig T W 1990 An introduction to martensite and shape memory *Engineering Aspects of Shape Memory Alloys* ed T W Duerig *et al* (London: Butterworth-Heinemann) pp 3–20
[19] Ugural A C and Fenster S K 2003 *Advanced Strength and Applied Elasticity* (New Jersey: Pearson Education)